PHOTONIC SENSORS / Vol. 9, No. 4, 2019: 317–326

Manipulation of Coherent Optical Propagation Based on Monolayer MoS_2 Resonator

Huajun CHEN*

School of Mechanics and Photoelectric Physics, Anhui University of Science and Technology, Huainan 232001, China

*Corresponding author: Huajun CHEN E-mail: chenphysics@126.com

Abstract: Atomically thin two-dimensional semiconductor nanomaterials have attained considerable attention currently. We here theoretically investigate the phenomena of slow and superluminal light based on the MoS_2 resonator system driven by two-tone fields. Superluminal and ultraslow probe light without absorption can be obtained via manipulating the pump laser on- and off-resonant with the exciton frequency under different parameters regimes, respectively, of which the magnitude is larger than that in a carbon nanotube resonator. The bandwidth of the probe spectrum determined by the quality factor Q of MoS_2 resonator is also presented. Furthermore, we also demonstrate the phenomenon of phonon induced transparency and show an optical transistor in the system. The all-optical device based on MoS_2 resonator may indicate potential chip-scale applications in quantum information with the currently popular pump-probe technology.

Keywords: MoS_2; nanomechanical resonator; fast and slow light; optical transistor

Citation: Huajun CHEN, "Manipulation of Coherent Optical Propagation Based on Monolayer MoS_2 Resonator," *Photonic Sensors*, 2019, 9(4): 317–326.

1. Introduction

Slow light effect [1] in ultracold atoms induced by electromagnetically induced transparency (EIT) [2] has been derived with numerous important developments in optical physics [3] and has inspired various potential applications [4]. Besides the phenomenon of slow light, superluminal phenomena are also observed in an atomic system [5] and a crystal structure [6]. At present, several schemes for obtaining slow light have also been proposed and realized, including coherent population oscillations in solids [7], stimulated Brillouin and Raman scattering in optical fibers [8], and wave-mixing in nematic liquid crystals [9]. Recently, cavity optomechanics which studies the interaction between light and mechanical oscillation [10] has become a rapidly developing field and plays an important role in many fields of physics, including gravitational-wave detectors [11], cooling of mechanical oscillators [12], and mass sensing [13]. Furthermore, the manipulation of light propagation, such as the slow and superluminal light, has also been investigated both theoretically and experimentally in optomechanical systems [14, 15], and one has been successfully observed an optically tunable delay of 50 ns with near-unity optical transparency, and superluminal light with a 1.4 μs signal advance [15].

On the other hand, atomically thin two-dimensional (2D) layered materials, such as monolayer molybdenum disulfide (MoS_2) with enormous stiffness, low density, intrinsically small size, and excellent mechanical properties, have

Received: 19 October 2018 / Revised: 6 January 2019

DOI: 10.1007/s13320-019-0535-z
Article type: Regular

attracted great interest recently due to their superior electrical-optical properties and potential applications [16]. MoS_2 is a semiconductor with the thickness-dependent electronic structure [17, 18], and with a decrease in the layer numbers of MoS_2, the material undergoes a transition from an indirect bandgap (1.2 eV in bulk) to a direct bandgap semiconductor (1.8 eV in monolayer) [19]. Monolayer MoS_2 has potential applications in photodetection [20, 21], photovoltaics [22], and MoS_2-based transistors [23, 24] due to this intrinsic property. Monolayer MoS_2 could be considered as the ultimate nanomaterials to structure micromechanical resonators, and additionally, multilayer MoS_2 nanomechanical resonator [25, 26] and single-layer MoS_2 mechanical resonator [27] have also been realized experimentally. It is noticed that although these significant impacts and immense applications based on monolayer/multilayer MoS_2 system have been demonstrated, the coherent optical propagation in MoS_2-based micromechanical resonator systems in all-optical domain has not been undertaken yet.

In this paper, we present a tunable slow- and fast-light device based on a platelike circular monolayer MoS_2 suspended on the Si/SiO_2 substrate [28] driven by two-tone fields. Due to the interaction of excition-phonon in the system, the probe laser will undergo a significant velocity change when applying a strong pump laser with a detuning under different parameters regimes, such as different exciton-resonator coupling and different resonance detuning. Adjusting the pump laser on- and off-resonance with the exciton frequency in the resonator, the probe laser group velocity undergoes fast light and slow light with little absorption. Furthermore, the linewidth of signal light spectrum is determined by the quality factor Q of MoS_2 resonator. The larger the quality factor of MoS_2 resonator is, the narrower the probe spectrum bandwidth is. In addition, electromagnetically induced absorption (EIA) and parametric amplification (PA) are also demonstrated with manipulating the pump field intensity, which may serve as a quantum optical transistor.

2. System and methods

Figure 1 gives the model based on monolayer MoS_2 [28, 29] with the optical pump-probe technology. Both experiments [30] and theories [31] have studied the vibrational properties of bulk, few layer, and monolayer MoS_2 recently. Although structural nonidealities and asymmetries of device based on MoS_2 nanostructures will occur and cause new mechanical resonances [32], for the sake of the analytical simplicity, we still take into account the model system as shown in Fig. 1 [25, 27]. In this suspended structure, the lowest-energy resonance corresponds to the fundamental flexural mode and the resonator is assumed to be characterized by sufficiently high quality factor Q. So the lifetime of the resonator is long enough. In this case, the new mechanical resonances caused by the edge effects and irregular shapes should be neglected compared with the fundamental flexural mode.

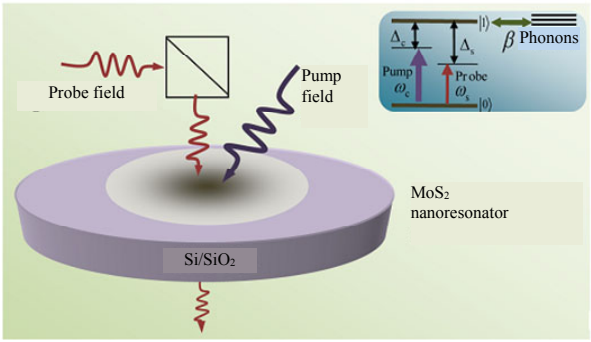

Fig. 1 Proposed setup of monolayer MoS_2-based nanomechanical resonator suspended on the Si/SiO_2 substrate with the optical pump-probe technique. The inset is the energy-level diagram of exciton in the MoS_2 coupled to the resonator.

We introduce the bosonic annihilation (creation) operator $b(b^+)$ to describe the eigenmode of the quantum harmonic oscillator, and $H_{\mathrm{NR}} = \hbar\omega_m(b^+b+1/2)$ is the Hamiltonian of the monolayer MoS_2 resonator with the frequency of the resonator ω_m. A two-level system with the ground state $|g\rangle$ and the first excited state (single exciton) $|e\rangle$ characterized by the pseudospin $-1/2$ operators

$S^{\pm}$ and S^z can be employed to describe the exciton since the monolayer MoS_2 is a direct bandgap semiconductor, and the inset is the energy level. The Hamiltonian of the localized two-level exciton can be written as $H_e = \hbar\omega_e S^z$ with the exciton frequency ω_e. The deformation potential interactions [13] induce the coupling between the exciton in monolayer MoS_2 resonator and the flexural motion, and therefore the interaction Hamiltonian between the resonator and the two-level exciton is $H_{\mathrm{NR}-e} = \hbar\omega_m \beta S^z (b^+ + b)$ with a coupling strength β. For the exciton-phonon interaction, symmetry-dependent exciton-phonon coupling in 2D and bulk MoS_2 observed by resonance Raman scattering has been investigated by Carvalho *et al.* [33]. They showed the A_{1g} phonon mode is enhanced by the A and B excitons, however, the enhancement decreases with a decreasing number of layers, due to the dependence of the lifetime of the intermediate excitonic states on the number of layers. Except the distinct exciton-phonon coupling can be explained considering the symmetries of the A_{1g} and E^1_{2g} phonons associated with the A, B, and C excitons, the symmetry-dependent exciton-phonon coupling can be also discussed using group theory arguments [32]. In addition, the electron-phonon coupling is also investigated by Raman and resonance Raman spectra of MoS_2 nanoparticles, and the electron-phonon coupling responsible for the strong-resonance conditions is identified through dynamic band calculations [34].

On the other hand, in the monolayer MoS_2 resonator system, there are multi-phonon modes exist in the system. Discussing all the phonon modes couple to the exciton is inefficient as the system size increases, and it is also unnecessary, because usually only a few modes or a signal mode within a small bandwidth is used for transmitting quantum states or quantum information processing. Therefore, we only consider the exciton and longitudinal optical phonons (LOPs) coupling in the system, and the optical propagation is investigated by the strong exciton-LOP interaction, in which the exciton behaves as an optical cavity and the phonon like a mechanical resonator analogy in a cavity optomechanics system.

The pump-probe technology [35] affords an effective method to investigate light-matter interaction. Applying the scheme to the monolayer MoS_2 resonator system, $H_{P-ex} = -\mu \sum_{i=c,s} E_i (S^+ \mathrm{e}^{-\mathrm{i}\omega_i t} + S^- \mathrm{e}^{\mathrm{i}\omega_i t})$ indicates the Hamiltonian of the exciton coupled to the two fields, where μ is the dipole moment of the exciton, and E_i is the slowly varying envelope of the field. In a rotating frame of the pump field frequency ω_c, we obtain the total Hamiltonian of the system as [28, 29]

$$H = \hbar\Delta_c S^z + \hbar\omega_m b^+ b + \hbar\omega_m \beta S^z (b^+ + b) - \mu E_c (S^+ + S^-) - \mu E_s (S^+ \mathrm{e}^{-\mathrm{i}\delta t} + S^- \mathrm{e}^{\mathrm{i}\delta t}) \quad (1)$$

where $\Delta_c = \omega_e - \omega_c$ and $\delta = \omega_s - \omega_c$ are the detuning of the pump frequency from the exciton frequency and probe frequency, respectively.

Writing the Heisenberg equations of motion and adding dissipation of the corresponding damping and noise terms, we obtain the following quantum Langevin equations as

$$\dot{S}^z = -\Gamma_1 (S^z + 1/2) + \mathrm{i}\Omega_c (S^+ - S^-) + \frac{\mathrm{i}\mu E_s}{\hbar} (S^+ \mathrm{e}^{-\mathrm{i}\delta t} - S^- \mathrm{e}^{\mathrm{i}\delta t}) \quad (2)$$

$$\dot{S}^- = -[\mathrm{i}(\Delta_c + \omega_m \beta N) + \Gamma_2] S^- + 2\mathrm{i}\Omega_c S^z - \frac{2\mathrm{i}\mu S^z E_s}{\hbar} \mathrm{e}^{-\mathrm{i}\delta t} + \hat{\tau}_{in}(t) \quad (3)$$

$$\ddot{N} + \gamma_m \dot{N} + \omega_m^2 N = -2\omega_m^2 \beta S^z + \hat{\varsigma}(t) \quad (4)$$

in which the position operator is $N = b^+ + b$, $\Gamma_1 (\Gamma_2)$ is the exciton relaxation rate (dephasing rate), $\gamma_m = \omega_m / Q$ is the decay rate of the resonator, and $\Omega_c = \mu E_c / \hbar$ is the Rabi frequency of the pump field. $\tau_{\mathrm{in}}(t)$ is the δ correlated Langevin noise operator with zero mean $\langle \tau_{\mathrm{in}}(t) \rangle = 0$ obeying the correlation function $\langle \tau_{\mathrm{in}}(t) \tau^+_{\mathrm{in}}(t') \rangle \sim \delta(t - t')$. The resonator mode is affected by a Brownian stochastic force with zero mean value, and $\varsigma(t)$

has the correlation function as [28]

$$\left\langle \hat{\varsigma}^{+}(t)\hat{\varsigma}(t')\right\rangle = \frac{\gamma_m}{\omega_m}\int \frac{d\omega}{2\pi}\omega \mathrm{e}^{-\mathrm{i}\omega(t-t')}\left[1+\coth\left(\frac{\hbar\omega}{2k_BT}\right)\right]$$

where k_B and T are the Boltzmann constant and the temperature of the reservoir, respectively.

Since the probe field is much weaker than the pump field, following the standard methods of quantum optics, the Heisenberg operator can be rewritten as the sum of its steady-state mean value and a small fluctuation with zero mean value: $O = O_0 + \delta O (O = S^z, S^-, N)$. The steady-state values are governed by the pump power and the small fluctuations by the probe power. In the steady state, disregarding the probe field, the time derivatives vanish, and the static solutions for the population inversion ($w_0 = 2S_0^z$) of the exciton obey the following algebraic equation $\Gamma_1(w_0+1)[\Gamma_2^2 + (\Delta_c - \beta^2\omega_m w_0)^2] + 4\Omega_c^2 w_0 \Gamma_2 = 0$. Keeping only the linear terms of the fluctuation operators, we make the ansatz [13] $\langle \delta O\rangle = O_+ \mathrm{e}^{-\mathrm{i}\delta t} + O_- \mathrm{e}^{\mathrm{i}\delta t}$. Solving the equation set and working to the lowest order in E_s but to all orders in E_c, we obtain the linear optical susceptibility as $\chi_{\mathrm{eff}}^{(1)}(\omega_s) = \mu S_+(\omega_s)/E_s = \Sigma_1 \chi^{(1)}(\omega_s)$ with $\Sigma_1 = \mu^2/\hbar\Gamma_2$, and $\chi^{(1)}(\omega_s)$ is given by

$$\chi^{(1)}(\omega_s) = \frac{\mathrm{i}(\Gamma_2 - \mathrm{i}\Delta_2)[S_0^*\Pi_1 - w_0(\Gamma_1 - \mathrm{i}\delta)]\Gamma_2 - w_0\Omega_c\Pi_2\Gamma_2}{[(\Gamma_1 - \mathrm{i}\delta)(\Gamma_2 - \mathrm{i}\Delta_2) - i\Omega_c\Pi_2](\mathrm{i}\Delta_1 + \Gamma_2) + \mathrm{i}\Omega_c\Pi_1(\Gamma_2 - \mathrm{i}\Delta_2)} \quad (5)$$

where $\chi = -2\omega_m^2\beta/\left(\omega_m^2 - \delta^2 - \mathrm{i}\delta\gamma_m\right)$, $\Delta_1 = \Delta_c - \delta + \omega_m\beta N_0$, $\Delta_2 = \Delta_c + \delta + \omega_m\beta N_0$, $\Pi_1 = -\mathrm{i}(\omega_m\beta S_0\chi + 2\Omega_c)$, $\Pi_2 = \mathrm{i}(\omega_m\beta S_0^*\chi + 2\Omega_c)$, $\Pi_3 = -\mathrm{i}(\omega_m\beta S_0\chi^* + 2\Omega_c)$, $\Pi_4 = \mathrm{i}(\omega_m\beta S_0^*\chi^* + 2\Omega_c)$. The imaginary and real parts of $\chi^{(1)}(\omega_s)$ indicate absorption and dispersion, respectively.

Based on the MoS_2 resonator system, we can determine the light group velocity as [36] $v_g = c/[n + \omega_s(dn/d\omega_s)]$ where $n \approx 1 + 2\pi\chi_{\mathrm{eff}}^1$. Therefore,

$$c/v_g = 1 + 2\pi \,\mathrm{Re}\,\chi_{\mathrm{eff}}^1(\omega_s)_{\omega_s=\omega_{ex}} + 2\pi\omega_s \,\mathrm{Re}(d\chi_{\mathrm{eff}}^1(\omega_s)/d\omega_s)_{\omega_s=\omega_{ex}}. \quad (6)$$

Obviously, when $\mathrm{Re}\,\chi_{\mathrm{eff}}^1(\omega_s)_{\omega_s=\omega_{ex}} = 0$, the dispersion is steeply positive or negative, and the group velocity is significantly reduced or increased. Thus we define the group velocity index n_g as

$$n_g = \frac{c}{v_g} - 1 = \frac{c - v_g}{v_g} = \frac{2\pi\omega_{ex}\rho\mu^2}{\hbar\Gamma_2}\mathrm{Re}\left(\frac{d\chi_{\mathrm{eff}}^{(1)}}{d\omega_s}\right)_{\omega_s=\omega_{ex}} = \Gamma_2\Sigma\,\mathrm{Re}\left(\frac{d\chi_{\mathrm{eff}}^{(1)}}{d\omega_s}\right)_{\omega_s=\omega_{ex}} \quad (7)$$

where $\Sigma = 2\pi\omega_{ex}\rho\mu^2/\hbar\Gamma_2$. One can observe the slow light when $n_g > 0$ and the superluminal light when $n_g < 0$ [37].

3. Results and discussion

The parameters of monolayer MoS_2 resonator are shown as follows [28, 29]: $\omega_m \approx 1.2$ GHz, $\Gamma_1 = 0.5$ GHz, $Q = 2000$, and $\beta = 0.1$. In Fig. 2(a), the imaginary part ($\mathrm{Im}\,\chi^{(1)}$) of linear optical susceptibility as function of probe-exciton detuning $\Delta_s = \omega_s - \omega_e$ at $\Delta_s = 0$ describes the absorption of the probe laser under two different exciton-resonator coupling strengths $\beta = 0.07$ and $\beta = 0.4$. Obviously, the intensity of the peaks is enhanced at the big exciton-resonator coupling strength. There are two sharp peaks locating at both sides of the spectrum that just corresponds to the vibrational frequency of the MoS_2 resonator, and the middle parts indicate the absorption of the exciton in the MoS_2 resonator. The phenomenon can be interpreted with a dressed-state picture. The two sharp peaks represent the resonance amplification and absorption of the vibrational mode of the MoS_2 resonator. The uncoupled two-level excition ($|g\rangle$ and $|e\rangle$) is dressed by the phonon mode *n* (*n* represents the number state of the phonon mode), and then the original eigenstates $|g\rangle$ and $|e\rangle$ are modified to form four dressed states, i.e. $|g, n\rangle$, $|g, n+1\rangle$, $|e, n\rangle$, and $|e, n+1\rangle$. The left sharp peak centered

at -1.2 GHz signifies the electron, making a transition from two low dressed levels ($|g, n\rangle$ and $|g, n+1\rangle$) to two high dressed levels ($|e, n\rangle$ and $|e, n+1\rangle$). The progress simultaneously absorbs two pump photons and emits a photon at $\omega_c - \omega_m$, thus amplifying a wave at $\Delta_s = -\omega_m$. The right sharp peak located at 1.2 GHz indicates the transition from $|g, n\rangle$ to $|e, n+1\rangle$ corresponding to the usual excitonic absorption resonance induced by the ac-Stark effect. The middle parts show the transition from $|g, n\rangle$ to $|e, n\rangle$ due to the MoS_2 resonator-induced stimulated Rayleigh resonance. We therefore present a straightforward optical scheme for determining the frequency of the resonator with the coherent optical spectrum. Fixing the control field detuning $\Delta_c = 0$ and scanning the probe frequency across the exciton frequency in the spectrum, we can easily and exactly obtain the vibration frequency of the MoS_2 resonator in all-optical domain.

Figure 2(b) shows the real part ($\mathrm{Re}\,\chi^{(1)}$) of linear optical susceptibility (i.e. the dispersion of the signal light) with a negative steep slope at $\Delta_s = 0$ with two different exciton-resonator coupling strengths $\beta = 0.07$ and $\beta = 0.4$, which signifies the potential for superluminal light achievement. In Figs. 2(c) and 2(d), we plot the group velocity index of probe laser n_g (in the unit of Π) as a function of the Rabi frequency Ω_c^2 at the exciton-resonator coupling strengths $\beta = 0.07$ and $\beta = 0.4$, respectively. We find that the output probe light can be about 10 times faster than input probe light in vacuum simply via tuning the pump laser on the resonant with exciton frequency in MoS_2 resonator system at $\beta = 0.07$ as shown in Fig. 2(c). However, when increasing the exciton-resonator coupling strength to $\beta = 0.4$, the evolution of group velocity index of probe laser n_g becomes more complicated as shown in Fig. 2(d), and there is a saltus with an increase in the Rabi frequency Ω_c^2.

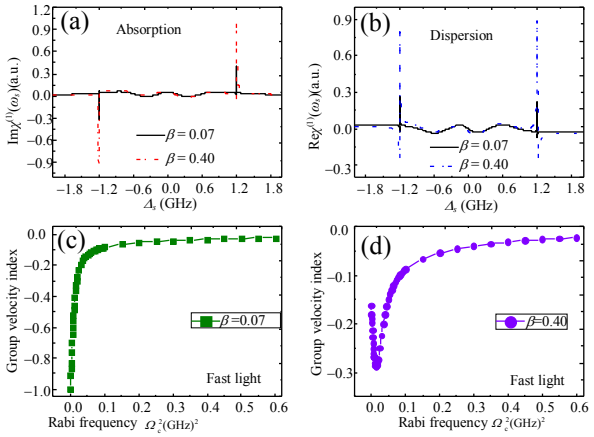

Fig. 2 Fast light based on the monolayer MoS_2 resonator system: (a) and (b) the dimensionless imaginary part ($\mathrm{Im}\,\chi_{\mathrm{eff}}^{(1)}$) and real part ($\mathrm{Re}\,\chi_{\mathrm{eff}}^{(1)}$) of the linear optical susceptibility (in units of Σ) as a function of the probe-exciton detuning Δ_s at the pump laser on-resonant with exciton frequency $\Delta_c = 0$ under two different exciton-resonator coupling strengths $\beta = 0.07$ and $\beta = 0.4$, respectively; (c) and (d) the group velocity index n_g of superluminal light (in units of Σ) as a function of pump Rabi frequency Ω^2 with two different exciton-resonator coupling strengths $\beta = 0.07$ and $\beta = 0.4$, respectively.

On the other hand, in the case of pump off resonant ($\Delta_c = \omega_m$), the imaginary part ($\mathrm{Im}\,\chi_{\mathrm{eff}}^{(1)}$) of linear optical susceptibility exhibits zero absorption at $\Delta_s = 0$ as shown in Fig. 3(a) under two different exciton-resonator coupling strengths ($\beta = 0.07$ and $\beta = 0.4$), which displays an analogous optomechanically-induced transparency [38] and termed as phonon-induced transparency (PIT) induced by the exciton-resonator coupling, and the phenomenon has been demonstrated in the coupled mechanical resonators system [39] and bilayer graphene nanoribbons [40]. Obviously, with an increase in the exciton-resonator coupling strength, the absorption spectrum splits into two peaks, which is analogous to the Rabi splitting of two-level systems in quantum optics and has a zero absorption point at $\Delta_s = 0$. Compared with the coupled mechanical resonators [39], the manufacturing process of the suspended monolayer MoS_2 nanomechanical resonator system is simple, and the frequency of the resonator can approach to gigahertz

(In [32], the frequency of the mechanical mode is about kilohertz). The realistic monolayer MoS_2 resonator can also exhibit a wide range of variations depending on its size-dependent parameters. Therefore, both the high and low frequencies of the mechanical resonator are allowed in the scheme. The so-called PIT appears in bilayer graphene nanoribbons induced by the plasmon excitation due to the coupling with the infrared active Γ-point optical phonon, and the function is more similar to that of the dark plasmon mode in the plasmon-induced transparency [40]. However, in the MoS_2 resonator system, the phenomenon of PIT is induced by the exciton-resonator coupling, and PIT will disappear immediately without the exciton-resonator coupling. For the essential of PIT, PIT in bilayer graphene nanoribbons [40] is derived from coherent destructive interference of excitation pathways, while in our scheme, the phenomenon of PIT is due to mechanically-induced coherent population oscillation when the pump-probe detuning equals the frequency of MoS_2 resonator [13]. Our demonstration opens an avenue for the exploration of slow light in this monolayer MoS_2 resonator system.

Figure 3(b) shows the dispersion (i.e. the real part $\mathrm{Re}\,\chi_{\mathrm{eff}}^{(1)}$) of the probe light in the condition of $\Delta_c=\omega_m$ with a positive steep slope at $\Delta_s=0$ under the exciton-resonator coupling strength $\beta=0.07$ and $\beta=0.4$, respectively, which indicates the potential of ultraslow light based on the coupled monolayer MoS_2 resonator system. Figures 3(c) and 3(d) exhibit the slow light curve at the exciton-resonator coupling strength $\beta=0.07$ and $\beta=0.4$, where the most slow light index can be produced in MoS_2 resonator device as 200 at $\Omega_c^2=0.05(\mathrm{GHz})^2$ and 156 at $\Omega_c^2=0.001(\mathrm{GHz})^2$, respectively. That is, the output signal pulse will be 200 and 156 times slower than the input light with a single MoS_2 resonator under two different coupling strengths. Compared with Fig. 3(c), the curve is steeper in Fig. 3(d) due to the stronger exciton-resonator coupling in the system. The physical origin of this result is the coupling between exciton and MoS_2 resonator vibration, which makes quantum interference between the MoS_2 resonator and the two optical fields via the exciton as $\delta=\omega_m$. Similar results in Fig. 3(c) have also been obtained in the carbon nanotube resonator, and the achieved slowdown of the group velocity in the MoS_2 nanoresonator is a bit higher than in the carbon nanotube resonator [41].

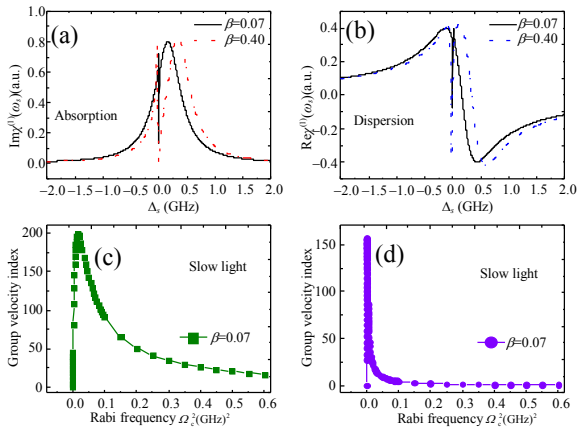

Fig. 3 Slow light based on the monolayer MoS_2 resonator system: (a) and (b) the dimensionless imaginary part and real part of the linear optical susceptibility (in units of Σ) as a function of the detuning Δ_s at the pump laser off-resonant with exciton frequency $\Delta_c=\omega_m$ under two different exciton-resonator coupling strengths $\beta=0.07$ and $\beta=0.4$, respectively; (c) and (d) the group velocity index n_g of slow light (in units of Σ) as a function of pump Rabi frequency Ω^2 with two different exciton-resonator coupling strengths $\beta=0.07$ and $\beta=0.4$, respectively.

In Fig. 4, we also make a comparison between the two conditions of $\Delta_c=\omega_m$ and $\Delta_c=-\omega_m$, and discuss the evolution of the group velocity index under two conditions as shown in Figs. 4(a) and 4(b). With controlling the change from the red sideband $\Delta_c=\omega_m$ to the blue sideband $\Delta_c=-\omega_m$, the group velocity index can realize the conversion from the slow light to the fast light. In addition, the fast light effect at $\Delta_c=-\omega_m$ is more complicated than the condition of $\Delta_c=0$ in Fig. 2(c), and it is more like the evolution in Fig. 2(d) under strength coupling.

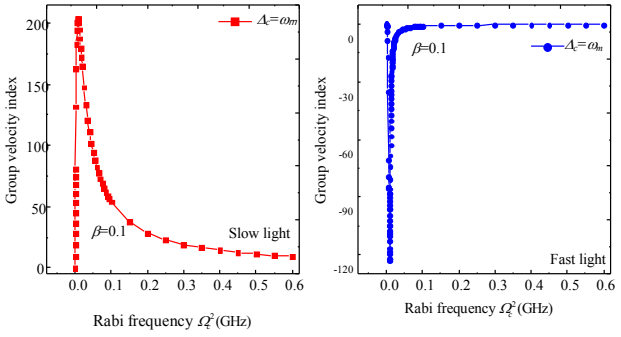

Fig. 4 Group velocity index n_g as a function of pump Rabi frequency Ω^2 under the two conditions of $\Delta_c = \omega_m$ and $\Delta_c = -\omega_m$ with the exciton-resonator coupling strengths $\beta = 0.1$.

Figure 5 displays the imaginary part of $\chi_{\text{eff}}^{(1)}$ as a function of Δ_s with three different quality factors Q of monolayer MoS_2 resonator. The inset shows the amplification of the most remarkable region of transparency. From this figure, we can demonstrate that the width of the signal spectrum decreases as the quality factor Q increases. Therefore, the larger the MoS_2 resonator quality factor is, the narrower of the probe spectrum width is. As a result, the MoS_2 resonator with high quality factor is beneficial to the transparency window. Due to the high quality factor (or short decay rate) of MoS_2 resonator, the slow light and fast light effect performed in MoS_2 is obviously better than that in other quantum systems such as quantum dots carbon nanotube resonator [41].

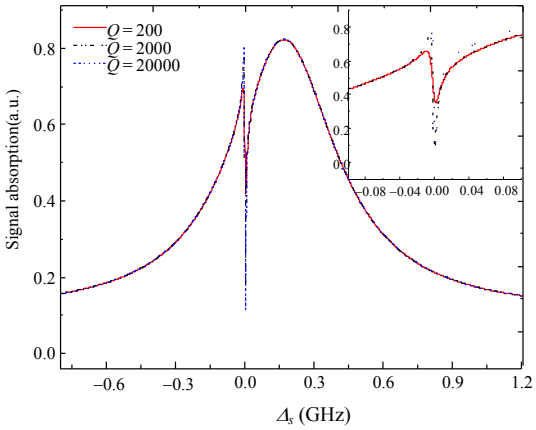

Fig. 5 Absorption spectrum of a probe field as a function of the detuning Δ_s with three different quality factors Q of MoS_2 resonator.

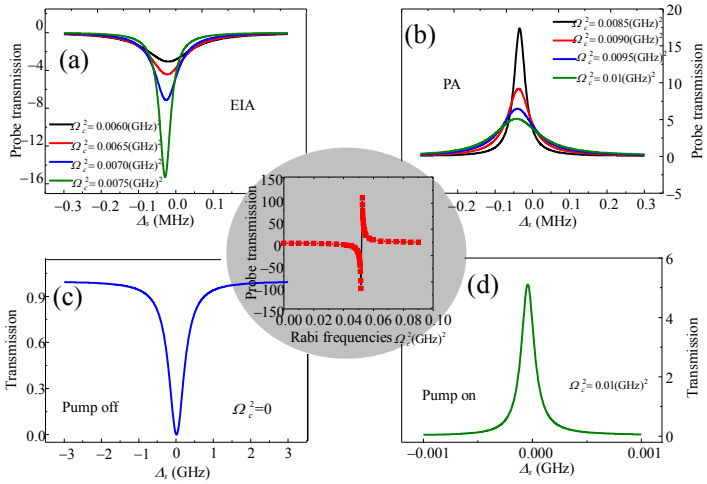

Fig. 6 Quantum optical transistor: (a) and (b) the probe transmission as a function of Δ_s with increasing Rabi frequencies of the pump field at $\Delta_c = -\omega_m$. The oval inset shows the relationship between the probe transmission and pump laser intensity; (c) and (d) attenuation and amplification of the probe laser when turning off and on the pump laser, respectively.

Switching the pump-exciton detuning to the blue sideband $\Delta_c = -\omega_m$ and increasing the pump field intensity, the probe transmission displays a deeper dip as shown in Fig. 6(a). In Fig. 6(a), the negative transmission of the probe laser with an increase in the pump intensity is the so-called electromagnetically induced absorption (EIA) [42]. However, with further increasing the pump laser

intensity, the system switches from EIA to parametric amplification (PA) resulting in the probe laser amplification as shown in Fig. 6(b), which has been demonstrated in the conventional optomechanical system [42]. The elliptical inset in Fig. 6 shows that there exists a turning point around $\Omega_c^2 = 0.008(\mathrm{GHz})^2$ which switches the probe transmission from EIA to PA. Therefore, the MoS_2 resonator system can not only switch the weak probe laser from off to on, but also serve as a quantum optomechanical transistor due to the probe amplifier effect. Turning off the pump laser, the weak probe laser displays the transmission spectrum owning to the usual exciton absorption resonance as shown in Fig. 6(c). However, turning on the pump laser and fixing the pump-exciton detuning $\Delta_c = -\omega_m$, the dip switches to a transmission peak immediately as shown in Fig. 6(d). This amplification comes from the quantum interference between the phonons and the beat of the two optical fields via the exciton in the MoS_2 resonator. Due to dressing with the phonon modes, the original two levels of exciton in the MoS_2 resonator system split into several metastable levels. When applying a strong pump laser to the system, the electrons can transit between the metastable levels, which induces the constructive interference, and eventually amplifies the weak probe laser.

4. Conclusions

We have theoretically investigated the coherent optical propagate based on monolayer MoS_2 nano-optomechanical system driven by two-tone fields. The dispersion of the probe light together with zero absorption indicates the potential for ultraslow light and the possibility of superluminal light based on the coupled monolayer MoS_2 resonator system with manipulating pump laser on- and off-resonant with exciton frequency in the resonator system. In addition, the bandwidth of the signal spectrum determined by the quality factor of monolayer MoS_2 resonator system is also demonstrated. Further, electromagnetically induced absorption and parametric amplification are demonstrated by the exciton-resonator coupling in the system, which may suggest a quantum optical transistor. Our study, therefore, will indicate a new avenue for fabricating nanomechanical resonator systems based on layered nanomaterials and such a tunable slow and fast light device based on graphene may have potential applications in optical networks and engineering in nanometer scale.

Acknowledgment

Huajun Chen is supported by the National Natural Science Foundation of China (Grant Nos. 11647001 and 11804004) and the Natural Science Foundation of Anhui Province (Grant No. 1708085QA11).

References

[1] L. V. Hau, S. E. Harris, Z. Dutton, and C. H. Behroozi, "Light speed reduction to 17 metres persecond in an ultracold atomic gas," *Nature*, 1999, 397(6720): 594–598.

[2] K. J. Boller, A. Imamoglu, and S. E. Harris, "Observation of electromagnetically induced transparency," *Physical Review Letters*, 1991, 66(20): 2593–2596.

[3] M. Fleischhauer, A. Imamoglu, and J. P. Marangos, "Electromagnetically induced transparency: optics in coherent media," *Review of Modem Physics*, 2005, 77(2): 633–673.

[4] M. D. Lukin, "Trapping and manipulating photon states in atomic ensembles," *Review of Modem Physics*, 2003, 75(2): 457–472.

[5] L. J. Wang, A. Kuzmich, and A. Dogariu, "gain-assisted superluminal light propagation," *Nature*, 2000, 406(6793): 277–279.

[6] M. S. Bigelow, N. N. Lepeshkin, and R. W. Boyd, "Superluminal and slow light propagation in a

room-temperature solid," *Science*, 2003, 301(5630): 200–202.

[7] P. C. Ku, F. Sedgwick, C. J. C. Hasnain, P. Palinginis, T. Li, H. Wang, *et al.*, "Slow light in semiconductor quantum wells," *Optics Letters*, 2004, 29(19): 2291–2293.

[8] Z. Zhu, D. J. Gauthier, and R. W. Boyd, "Stored light in an optical fiber via stimulated Brillouin scattering," *Science*, 2007, 318(5857): 1748–1750.

[9] S. Residori, U. Bortolozzo, and J. P. Huignard, "Slow and fast light in liquid crystal light valves," *Physical Review Letters*, 2008, 100(20): 203603-1–203603-2.

[10] M. Aspelmeyer, T. J. Kippenberg, and F. Marquardt, "Cavity optomechanics," *Review of Modem Physics*, 2014, 86(4): 1391–1455.

[11] A. Abramovici, W. E. Althouse, R. W. Drever, Y. Gürsel, S. Kawamura, F. J. Raab, *et al.*, "LIGO: the laser interferometer gravitational-wave observatory," *Science*, 1992, 256(5055): 325–333.

[12] A. Naik, O. Buu, M. D. LaHaye, A. D. Armour, A. A. Clerk, M. P. Blencowe, *et al.,* "Cooling a nanomechanical resonator with quantum back-action," *Nature*, 2006, 443(7108): 193–196.

[13] J. J. Li and K. D. Zhu, "All-optical mass sensing with coupled mechanical resonator systems," *Physics Reports*, 2013, 525(3): 223–254.

[14] B. Chen, C. Jiang, and K. D. Zhu, "Slow light in a cavity optomechanical system with a Bose-Einstein condensate," *Physics Review A*, 2011, 83(5): 055803-1–055803-4.

[15] A. H. S. Naeini, T. P. Alegre, J. Chan, M. Eichenfield, M. Winger, Q. Lin, *et al.*, "Electromagnetically induced transparency and slow light with optomechanics," *Nature*, 2011, 472(7341): 69–73.

[16] R. Ganatra and Q. Zhang, "Few-layer MoS_2: a promising layered semiconductor," *ACS Nano*, 2014, 8(5): 4074–4099.

[17] K. F. Mak, C. Lee, J. Hone, J. Shan, and T. F. Heinz, "Atomically thin MoS_2: a new direct-gap semiconductor," *Physical Review Letters*, 2010, 105(13): 136805-1–136805-4.

[18] K. He, C. Poole, K. F. Mak, and J. Shan, "Experimental demonstration of continuous electronic structure tuning via strain in atomically thin MoS_2," *Nano Letters*, 2013, 13(6): 2931–2936.

[19] G. Eda, H. Yamaguchi, D. Voiry, T. Fujita, M. Chen, and M. Chhowalla, "Photoluminescence from chemically exfoliated MoS_2," *Nano Letters*, 2011, 11(12): 5111–5116.

[20] H. S. Lee, S. W. Min, Y. G. Chang, M. K. Park, T. Nam, H. Kim, *et al.*, "MoS_2 nanosheet phototransistors with thickness-modulated optical energy gap," *Nano Letters*, 2012, 12(7): 3695–3700.

[21] O. L. Sanchez, D. Lembke, M. Kayci, A. Radenovic, and A. Kis, "Ultrasensitive photodetectors based on monolayer MoS_2," *Nature Nanotechnology*, 2013, 8(7): 497–501

[22] M. Fontana, T. Deppe, A. K. Boyd, M. Rinzan, A. Y. Liu, M. Paranjape, *et al.*, "Electron-hole transport and photovoltaic effect in gated MoS_2 Schottky junctions," *Scientific Reports*, 2013, 3: 1634-1–1634-5.

[23] B. Radisavljevi´c, A. Radenovi´c, J. Brivio, V. Giacometti, and A. Kis, "Single-layer MoS_2 transistors," *Nature Nanotechnology*, 2011, 6(3): 147–150.

[24] D. Krasnozhon, D. Lembke, C. Nyffeler, Y. Leblebici, and A. Kis, "MoS_2 transistors operating at gigahertz frequencies," *Nano Letters*, 2014, 14(10): 5905–5911.

[25] J. Lee, Z. Wang, K. He, J. Shan, and X. L. Feng, "High frequency MoS_2 nanomechanical resonators," *ACS Nano*, 2013, 7(7): 6086–6091.

[26] R. V. Leeuwen, A. C. Gomez, G. A. Steele, H. S. J. V. D. Zant, and W. J. Venstra, "Time-domain response of atomically thin MoS_2 nanomechanical resonators," *Applied Physics Letters*, 2014, 105(4): 041911-1–041911-3.

[27] A. C. Gomez, R. V. Leeuwen, M. Buscema, H. S. J. V. D. Zant, G. A. Steele, and W. J. Venstra, "Single-layer MoS_2 mechanical resonators," *Advanced Materials*, 2013, 25(46): 6719–6723.

[28] H. J. Chen and K. D. Zhu, "Coherent optical responses and their application in biomolecule mass sensing based on a monolayer MoS_2 nanoresonator," *Journal of the Optical Society of America B*, 2014, 31(7): 1684–1690.

[29] J. B. Li, S. Xiao, S. Liang, M. D. He, N. C. Kim, Y. Luo, *et al.*, "Switching freely between superluminal and subluminal light propagation in a monolayer MoS_2 nanoresonator," *Optics Express*, 2017, 25(12): 13567–13576.

[30] C. Lee, H. Yan, L. E. Brus, T. F. Heinz, J. Hone, and S. Ryu, "Anomalous lattice vibrations of single-and few-layer MoS_2," *ACS Nano*, 2010, 4(5): 2695–2700.

[31] T. Li, "Ideal strength and phonon instability in single-layer MoS_2," *Physical Review B*, *Condensed Matter*, 2012, 85(23): 235407.

[32] Z. Wang, J. Lee, K. He, J. Shan, and P. X. L. Feng, "Embracing structural nonidealities and asymmetries in two-dimensional nanomechanical resonators," *Scientific Reports*, 2014, 4: 3919–3925.

[33] B. R. Carvalho, L. M. Malard, J. M. Alves, C. Fantini, and M. A. Pimenta, "Symmetry-dependent exciton-phonon coupling in 2D and bulk MoS_2 observed by resonance Raman scattering," *Physical Review Letters*, 2015, 114(13): 136403-1–36403-5.

[34] G. L. Frey, R. Tenne, M. J. Matthews, M. S. Dresselhaus, and G. Dresselhaus, "Raman and resonance Raman investigation of MoS2 nanoparticles," *Physical Review B*, 1999, 60(4): 2883–2892.

[35] X. Xu, B. Sun, P. R. Berman, D. G. Steel, A. S. Bracker, D. Gammon, *et al.*, "Coherent optical spectroscopy of a strongly driven quantum dot," *Science*, 2007, 317(5840): 929–932

[36] S. E. Harris, J. E. Field, and A. Kasapi, "Dispersive properties of electromagnetically induced transparency," *Physical Review A*, 1992, 46(1): R29–R32.

[37] R. W. Boyd and D. J. Gauthier, "Controlling the velocity of light pulses," *Science*, 2009, 326(5956): 1074–1077.

[38] A. H. S. Naeini, T. M. Alegre, J. Chan, M. Eichenfield, M. Winger, Q. Lin, *et al.*, "Electromagnetically induced transparency and slow light with optomechanics," *Nature*, 2011, 472(7341): 69–73.

[39] H. Okamoto, A. Gourgout, C. Y. Chang, K. Onomitsu, I. Mahboob, E. Y. Chang, *et al.*, "Coherent phonon manipulation in coupled mechanical resonators," *Nature Physics*, 2013, 9(8): 480–484.

[40] H. Yan, T. Low, F. Guinea, F. Xia, and P. Avouris, "Tunable phonon-induced transparency in bilayer graphene nanoribbons," *Nano Letters*, 2014, 14(8): 4581–4586.

[41] J. J. Li and K. D. Zhu, "Tunable slow and fast light device based on a carbon nanotube resonator," *Optics Express*, 2012, 20(6): 5840–5848.

[42] A. H. S. Naeini, A. T. P. Mayer, J. Chan, M. Eichenfield, M. Winger, Q. Lin, *et al.*, "Electromagnetically induced transparency and slow light with optomechanics," *Nature*, 2014, 472: 69–73.